DOI: 10.1002/chem.200800286

A Feasibility Study on the Use of $Li_4V_3O_8$ as a High Capacity Cathode Material for Lithium-Ion Batteries

See-How Ng,[a] Nicolas Tran,[a] Kirill G. Bramnik,[b] Hartmut Hibst,[c] and Petr Novák*[a]

Abstract: $Li_4V_3O_8$ materials have been prepared by chemical lithiation by Li_2S of spherical $Li_{1.1}V_3O_8$ precursor materials obtained by a spray-drying technique. The over-lithiated vanadates were characterised physically by using scanning electron microscopy (SEM) and X-ray diffraction (XRD), and electrochemically using galvanostatic charge-discharge and cyclic voltammetry measurements in both the half-cell (vs. Li metal) and full-cell (vs. graphite) systems. The $Li_4V_3O_8$ materials are stable in air for up to 5 h, with almost no capacity drop for the samples stored under air. However, prolonged exposure to air will severely change the composition of the $Li_4V_3O_8$ materials, resulting in both $Li_{1.1}V_3O_8$ and Li_2CO_3. The electrochemical performance of these over-lithiated vanadates was found to be very sensitive to the conductive additive (carbon black) content in the cathode. When sufficient carbon black is added, the $Li_4V_3O_8$ cathode exhibits good cycling behaviour and excellent rate capabilities, matching those of the $Li_{1.1}V_3O_8$ precursor material, that is, retaining an average charge capacity of 205 mAh g^{-1} at 2800 mA g^{-1} (8C rate; 1C rate means full charge or discharge of a battery in one hour), when cycled in the potential range of 2.0–4.0 V versus Li metal. When applied in a non-optimised full cell system (vs. graphite), the $Li_4V_3O_8$ cathode showed promising cycling behaviour, retaining a charge capacity (Li^+ extraction) above 130 mAh g^{-1} beyond 50 cycles, when cycled in the voltage range of 1.6–4.0 V, at a specific current of 117 mA g^{-1} (C/3 rate).

Keywords: cathode • electrochemistry • full cell electrochemistry • high-capacity lithiation • lithium-ion batteries • over-lithiated vanadates

Introduction

Electrochemical energy conversion and storage devices undoubtedly have a major role to play in the new clean energy economy. There are probably two dominant types of energy storage systems required for the new energy economy: one related to static load levelling of renewables, and the other related to transport. For both, cost and reliability are extremely important; energy and power density are also important, although to differing degrees. For energy storage related to transport, high-power batteries are being developed for hybrid electric vehicles. Amongst the available energy storage systems, the lithium-based rechargeable battery system is of particular interest for hybrid electric vehicle applications. Of all the rechargeable battery systems, the lithium-ion (Li-ion) battery possesses the greatest energy density and has a power density close to that of the nickel–cadmium (Ni–Cd) battery.[1,2]

However, despite their outstanding commercial success, these batteries are still open to improvements. In particular, improvements to the positive electrode are critical for the progress of lithium-ion batteries. Indeed, considerable efforts are presently directed towards the replacement of the high-cost, partially toxic $LiCoO_2$ with more affordable and sustainable materials. Vanadium oxides such as V_2O_5, V_6O_{13} and LiV_3O_8 appeared to be promising candidates as positive electrode materials due to the advantages of higher capacity, lower cost, and better safety features.[3–8] However, these materials are not suitable for use in today's lithium-ion batteries, because they deliver no extractable lithium ions during the first charge.

Chemical lithiation of vanadium oxides for producing viable positive electrodes at an economical scale is indeed a scientific and industrial challenge. Previous lithiation methods based on wet chemistry, in particular with LiI (in aceto-

---

[a] Dr. S.-H. Ng, Dr. N. Tran, Dr. P. Novák
Paul Scherrer Institut, Electrochemistry Laboratory
5232 Villigen PSI (Switzerland)
Fax: (+41) 56-310-4415
E-mail: petr.novak@psi.ch

[b] Dr. K. G. Bramnik
BASF SE, Performance Chemicals Research
67056 Ludwigshafen (Germany)

[c] Prof. Dr. H. Hibst
BASF SE, Research Chemicals and Technology
67056 Ludwigshafen (Germany)

nitrile)[9] and nBuLi (in hexane),[10] have proven not to be economically attractive. Another lithiation technique based on electrochemical reduction was suggested, but was also deemed ineffective and expensive.[11,12] Recently, Barker and co-workers[13] proposed an economical lithiation method based on a rapid, single-step carbothermal reduction (CTR) approach to synthesise γ-LiV_2O_5. Unfortunately, the maximum amount of lithium that could be electrochemically extracted was only 0.92 moles, which translates to a maximum reversible specific capacity of 130 $mAh\,g^{-1}$. A higher capacity is needed to compensate for the lower operating voltage ($\approx$3 V) for vanadium-based positive electrodes to attain a high energy density for the battery.

One possible solution would be to synthesize a $Li_{1+x}V_3O_8$ ($2<x<4$) compound for which a theoretical reversible specific capacity above 200 $mAh\,g^{-1}$ is achievable.[14–16] Herein, we report on an inexpensive and industrially scalable method for producing $Li_4V_3O_8$ using a spray-drying method to produce the $Li_{1.1}V_3O_8$ precursor materials in the first instance,[17] followed by chemical lithiation of the precursor materials with Li_2S in acetonitrile.[18] Systematic characterisations of the lithiated vanadates in terms of their physical properties (XRD and SEM) as well as their electrochemical performance are discussed in detail. In addition, a comprehensive feasibility study of these over-lithiated vanadates when applied as cathodes in the Li-ion battery full-cell configuration is presented.

Results and Discussion

The determined Li/V ratio was 3.80(5)/3.00(5) for the as-synthesised $Li_4V_3O_8$ material, which is in good agreement with the nominal value (4/3) when considering the accuracy of the analytical method for each element. Therefore, $Li_4V_3O_8$ will be used as the common term throughout the text because it has been shown in the literature[16] that the chemical or electrochemical insertion of Li occurs in two phases $Li_{1+x}V_3O_8$: from $x=a$ to $x=1.9$, Li is inserted in the single phase $Li_{1+a}V_3O_8$; and from $x=3$ to $x=4$, Li is inserted in the single phase $Li_4V_3O_8$. In between, the mechanism is a two-phase process with the transformation from $Li_{2.9}V_3O_8$ to $Li_4V_3O_8$. Hereafter, the latter transformation is called "Li3–Li4 transition". For our compound, the x value was determined to be approximately 2.8 by inductively coupled plasma optical emission spectrometry (ICP-OES) measurement. Therefore, our compound definitely consists of two phases. Thus, the reason for the use of $Li_4V_3O_8$ in this paper is actually an average value based on the ICP-OES measurements.

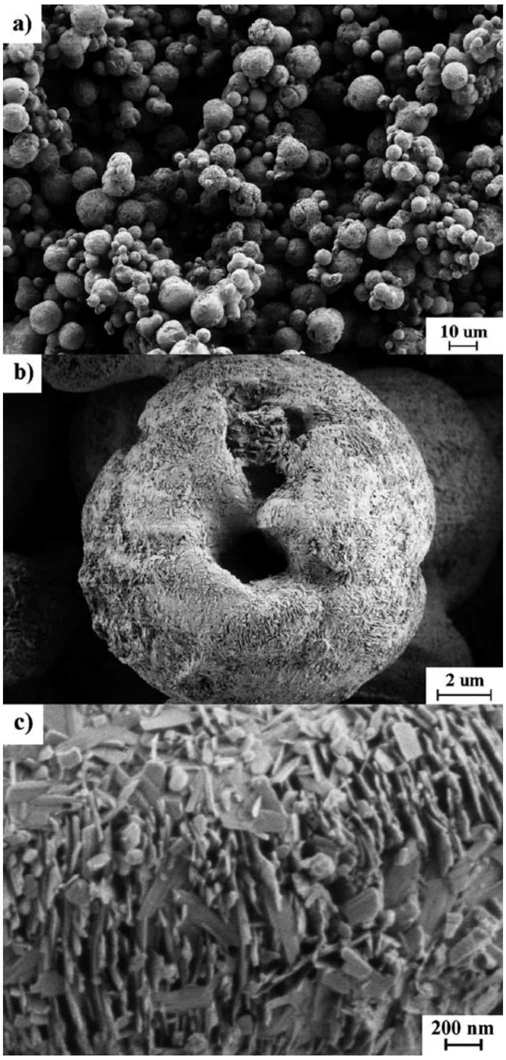

Figure 1. SEM images of the as-synthesised $Li_4V_3O_8$ material at different magnifications.

Figure 1 shows an SEM image of the as-synthesised $Li_4V_3O_8$ particles, which are mainly macro-sized (up to 20 μm, see Figure 1 a), dense, spherical agglomerates (see Figure 1 b) consisting of rod-like nanostructures (100–150 nm wide) as their building blocks (see Figure 1 c). This observation is consistent with those reported for the spray-dried $Li_{1.1}V_3O_8$ precursor material,[17] and is also a general type of morphology normally obtained for spray-dried composite materials in air.[19,20] Thus we could conclude that the chemical lithiation process did not alter the morphology of the precursor material.

One of the most important challenges for an over-lithiated compound is to display stability in an ambient environment, due to the risk of oxidation of the as-synthesised materials in air. To test the stability of the as-synthesised $Li_4V_3O_8$ compound when exposed to ambient air, both long- and short-term storage-in-air tests were performed with the as-synthesised $Li_4V_3O_8$ compound for both the powder and electrode forms. For the long-term tests, after six months of storage in ambient conditions (see Figure 2), the as-synthesised $Li_4V_3O_8$ compound, which previously consisted of two coexisting phases ($Li_{2.7}V_3O_8$ and $Li_{4.8}V_3O_8$),[16] had been oxidised and converted to both $Li_{1.1}V_3O_8$[21] and Li_2CO_3 (JCPDS Card No. 22–1141). The *hkl* indices listed in Figure 2 are based on the monoclinic phase, $Li_{1.1}V_3O_8$ structure (JCPDS Card No. 72–1193) reported by Wadsley in

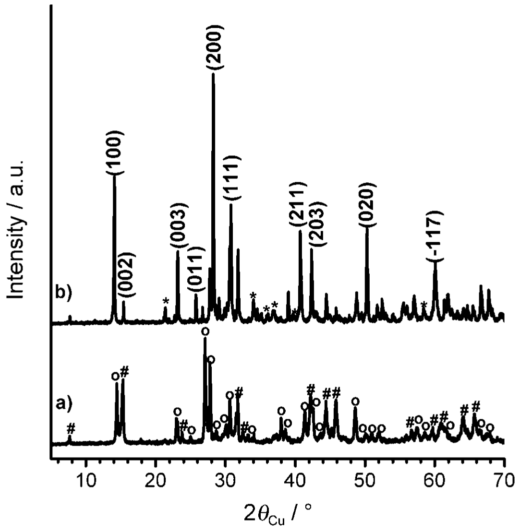

Figure 2. X-ray diffraction (XRD) patterns of the $Li_4V_3O_8$ material: a) as-synthesised, and b) after storage under ambient air for six months. The *hkl* indices are indicated in parentheses (based on JCPDS Card No. 72–1193 for $Li_{1.1}V_3O_8$ compound). Peaks that correspond to $Li_{2.7}V_3O_8$, $Li_{4.8}V_3O_8$, and Li_2CO_3, are noted as (o), (#), and (*), respectively.

1957.[21] In general, our statement for the oxidation of $Li_4V_3O_8$ is based on the refinement of the XRD pattern. We believe that the phase with $a = 0.1$ is formed according to the refined lattice parameters, which are close to those mentioned by Wadsley et al.[21]

Another proof of oxidation after prolonged storage in air was the increase of mass for the as-synthesised $Li_4V_3O_8$ material with time of storage. As seen from Figure 3, an increase of approximately 20 wt% is recorded after more than six months of storage (> 200 days) in ambient conditions. This weight increase can be explained by water and CO_2 uptake from the air and the formation of a Li_2CO_3 layer (see Figure 2b). Note that our experimental measurement of mass changes for the unlithiated $Li_{1.1}V_3O_8$ precursor material showed a negligible increase in mass (<1 wt%) even after six months of storage in ambient air, which shows that the over-lithiated $Li_4V_3O_8$ material is more sensitive.

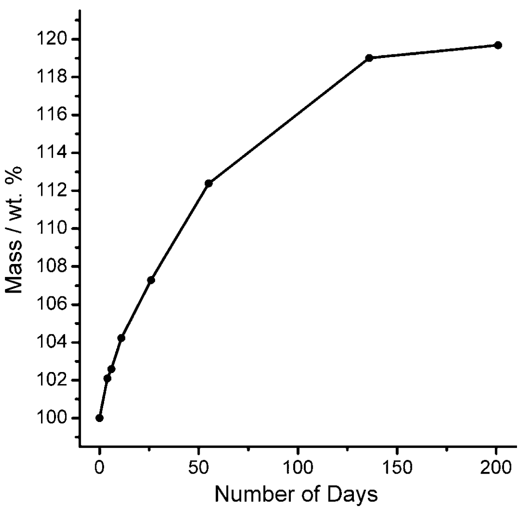

Figure 3. Increase of mass for the as-synthesised $Li_4V_3O_8$ material (in powder form) as a function of storage time under ambient air.

Hence, for the short-term tests, it was of great significance for industrial applications to gauge the extent of oxidation of the as-synthesised $Li_4V_3O_8$ material, to prevent the loss of electrochemical activity and available lithium due to the formation of an insulating Li_2CO_3 layer on the surface of the active $Li_4V_3O_8$ material when exposed to air. To evaluate the effect of the cathode material's oxidation in air towards the overall electrochemical activity, $Li_4V_3O_8$ cathodes were dried in air after doctor-blading, and exposed to ambient air for various time durations. Figure 4 shows that the $Li_4V_3O_8$ cathodes could maintain almost 100% of their average charge capacities over 10 cycles (at C/3 rate) when exposed to ambient air for approximately five hours. This should provide ample handling time for practical industrial applications in ambient atmosphere, or possibly an even longer period of time if manufactured under dry-room conditions.

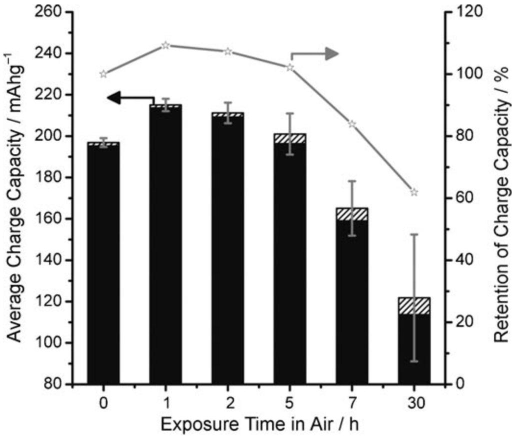

Figure 4. Average (over 10 cycles) and percentage of retained charge capacities of the $Li_4V_3O_8$ electrodes with 50 wt% active mass after exposure to ambient air for various lengths of time. Cycling took place between 2.0 and 3.3 V at 117 mA g^{-1} (C/3 rate). The solid columns represent the galvanostatic part of the total capacities, and the patterned columns indicate the contribution from the potentiostatic part of the total capacities.

Actually, Li_2CO_3 has been suggested as an additive (or coating) for oxide electrodes to provide additional safety measures (anti-overcharging) and to "catch" and neutralise any hydrofluoric acid (HF) generation due to electrolyte decomposition.[22–24] It is possible, therefore, that a small amount of Li_2CO_3 in the $Li_4V_3O_8$ material (in this case less than 2 wt%) could be favourable. Note that Li_2CO_3 is disadvantageous for carbon dioxide development from oxide electrodes at high potentials,[24] but the working potential window for vanadates (<4 V vs. Li/Li^+) is well below the relevant potential limit.

The total capacity shown in Figure 4 corresponds to the cumulative capacity of the galvanostatic part and the potentiostatic part. However, importantly, normally only the galvanostatic part of the capacity is relevant for practical applications.

Having considered the stability of these over-lithiated vanadate materials when exposed to ambient air, the next question is about their electrochemical activity when applied as cathodes in lithium-ion batteries. To gauge independently the electrochemical properties of the as-synthesised $Li_4V_3O_8$ material, influences from electrode engineering should be kept to a minimum.

One of the key factors in electrode engineering is the amount of conductive additive (carbon black in this case) needed in the cathode to ensure a homogeneous electrical connection between the active electrode materials ($Li_4V_3O_8$ in this case).[25–29] As seen from Figure 5, when the amount of carbon black (CB) added was increased from 10.5 wt% (see Figure 5 a) to 43.0 wt% (see Figure 5 b), the charge capacity ratio, Q_c, (ratio of galvanostatic charge over total charge) was maintained above 98% beyond 30 cycles for the latter case, whereas, in the former case, the charge capacity ratio dropped significantly with cycling to less than 68% after 30 cycles.

Panero et al. have reported that the resistivity of the $Li_{1+x}V_3O_8$ material increases upon increasing lithiation (for high x value).[30] Therefore, it is essential that a sufficient amount of conductive additive is added for good performance (up to 30%).[30] As a result, all subsequent electrochemical measurements conducted for the $Li_4V_3O_8$ cathodes are performed using 50 wt% active electromaterials (or 43 wt% CB).

Another important cycling characteristic related to electrode engineering is the cut-off potential for the overall working voltage of a lithium-ion battery system. Because the cathode plays an important role in lithium extraction (or de-insertion), for it to act as a source of lithium, the charging characteristics will be the focus. Therefore, the cut-off potential for the charging step will be investigated here. Figure 6 shows the retention of the specific charge capacities with cycling for two different cut-off potentials, that is, 3.3 and 4.0 V versus Li/Li^+. We can see clearly that, after 50 cycles, the charge capacity retention was increased from 78% to 86% when the cut-off potential was increased from 3.3 to 4.0 V. A possible explanation of this effect could be the changing of the lithium extraction mechanism during cycling: long-term cycling leads to the shifting of the potential of one de-intercalation reaction of the multi-step Li extraction process to a higher voltage, [30–33] resulting in incomplete Li extraction for the cell cycled with the cut-off voltage of 3.3 V. Pistoia et al.[30–33] also reported that only 80% of the capacity for the first charge could be recovered when charging to 3.3 V versus Li/Li^+. The remaining capacity could be recovered by extending the charge limit above 3.8 V versus Li/Li^+. Although the difference is not huge, this additional

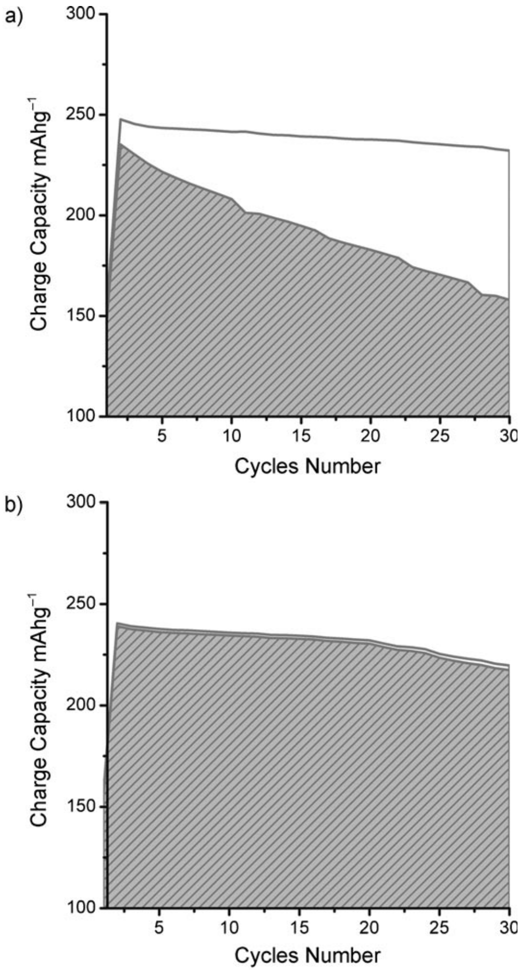

Figure 5. The charge capacities of the $Li_4V_3O_8$ electrodes containing different amounts of active mass: a) 86 wt% $Li_4V_3O_8$, and b) 50 wt% $Li_4V_3O_8$. Cycling took place between 2.0 and 3.3 V at 117 mA g^{-1} (C/3 rate). The white areas represent the total Li^+ extraction capacities, and the patterned areas indicate the galvanostatic part of the total Li^+ extraction capacities.

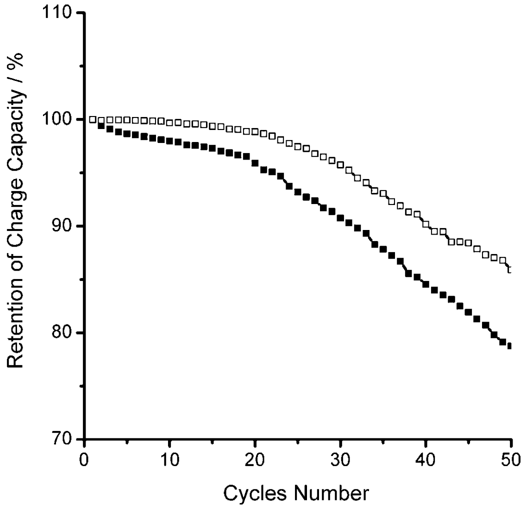

Figure 6. The cycling performance of the $Li_4V_3O_8$ electrodes with 50 wt% active mass when cycled at different cut-off potentials. The specific current applied was 117 mA g^{-1} (C/3 rate). (■ 2.0–3.3 V, □ 2.0–4.0 V).

capacity retention from the 3.3–4.0 V range contributes not only to an increase in the specific charge capacity but also to a higher overall working voltage for the lithium-ion battery, which would result in a higher energy density for the battery system. Note that the stability window of the unlithiated $Li_{1.1}V_3O_8$ precursor material is different.[17,34–36]

In fact, we are confident about the strong influence of electrode engineering on the electrochemical performance of the $Li_4V_3O_8$ cathode materials (see Figure 5); the next question is on the rate capability of these over-lithiated vanadates. As demonstrated in Figure 7, when applied in the half-cell (vs. Li metal), the $Li_4V_3O_8$ electrodes exhibited rather high average specific capacities, retaining 235 mAh g^{-1} (Li^+ extraction) and 233 mAh g^{-1} (Li^+ insertion) when cycled in the potential range of 2.0–3.3 V (see Figure 7a), and 279 mAh g^{-1} (Li^+ extraction) and 283 mAh g^{-1} (Li^+ insertion) when cycled in the potential range of 2.0–4.0 V (see Figure 7b), at a specific current of 117 mA g^{-1} (C/3 rate). Furthermore, the $Li_4V_3O_8$ electrodes also demonstrated excellent rate capabilities, matching those of the $Li_{1.1}V_3O_8$ precursor material, retaining an average specific charge capacity of 205 mAh g^{-1} at 2800 mA g^{-1} (8C rate), when cycled in the potential range of 2.0–4.0 V versus Li metal (see Figure 7b).

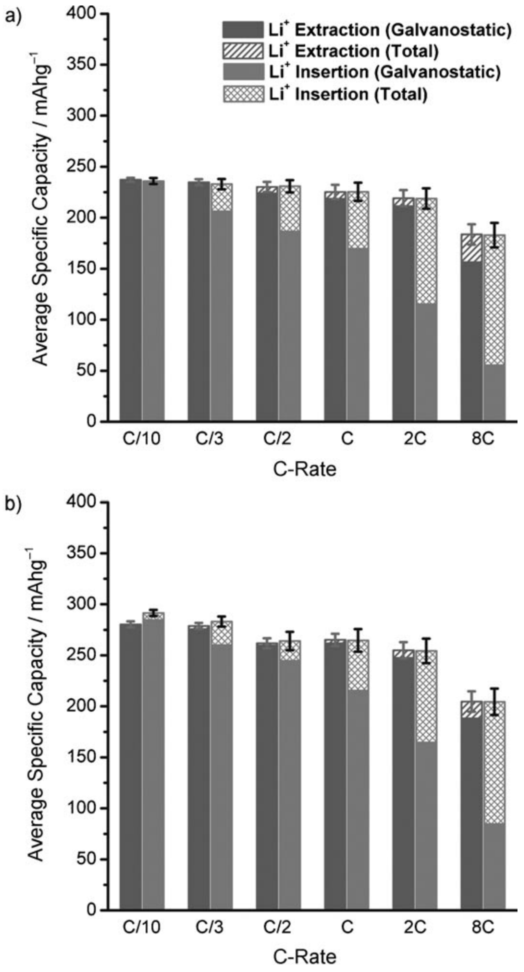

Figure 7. The average (over 10 cycles) capacities of the $Li_4V_3O_8$ electrodes (50 wt % active mass) cycled at different specific currents (C-rates) for different cut-off potentials: a) 2.0–3.3 V (vs. Li/Li^+), and b) 2.0–4.0 V (vs. Li/Li^+). Note that 1C rate is assumed to be 350 mA g^{-1} in all cases.

The capacity contribution from the galvanostatic part decreased significantly with increasing C-rate during insertion of Li ions. This could be attributed to the slower Li^+ migration from the surface to the inside of the electrode when the concentration of Li^+ on the electrode-electrolyte surface is high at higher C-rate.[17,18] In addition, the charge capacity ratios, Q_c, at high C-rates were also higher when the cut-off potential was increased from 3.3 to 4.0 V vs. Li metal. This could be due to the increase in electrochemical driving force towards oxidation (charging step) since the potential difference was increased from $(3.3-E)$ V to $(4.0-E)$ V, where E is the thermodynamic potential (vs. Li/Li^+) of the oxide electrode.[37]

As mentioned in the Introduction, the main objective of this research work was to produce an over-lithiated vanadate material that could provide lithium ions during the first charge when applied as the cathode in Li-ion rechargeable batteries. This leads us to the next important issue: the feasibility of this $Li_4V_3O_8$ material as a high capacity cathode material when applied in a full-cell Li-ion battery system configuration with a conventional graphite electrode as the anode. To illustrate the electrochemical characteristics of a full-cell system, Figure 8 shows typical first cycle charge-discharge curves for both the individual cathode ($Li_4V_3O_8$ in this case) and anode (LBG1025 graphite in this case) plotted with a normalised time frame (or similar C-rate). As can be deduced from Figure 8, the plausible working region for the operating cell voltage is between 1.6 and 4.0 V. In order

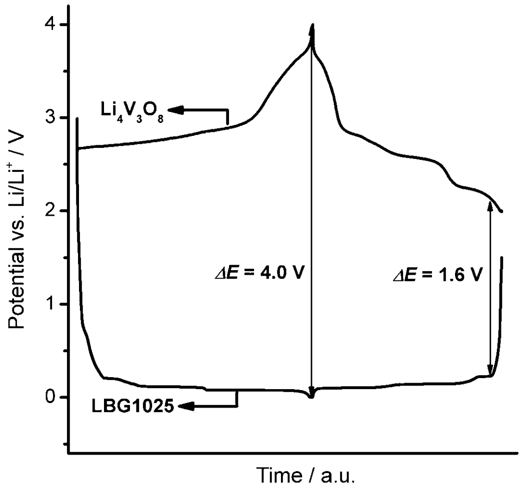

Figure 8. Typical first cycle charge-discharge curves of the individual working electrodes ($Li_4V_3O_8$ and LBG1025 graphite) when cycled against a Li metal counter electrode. Note that the plot is normalised to the same time scale (C-rate) for both working electrodes and the voltage difference is given by ΔE.

to ensure complete charging of the full cell system, the graphite anode is present in excess of active mass (>5–10 wt%). Please note that this is a non-optimised electrode configuration for a full-cell system.

When applied in a non-optimised full-cell system (vs. LBG1025 graphite), the $Li_4V_3O_8$ electrode showed promising cycling behaviour (see Figure 9), retaining a charge capacity (Li^+ extraction) above 130 mAh g^{-1} and also a charge efficiency above 98% after 50 charge-discharge cycles, when cycled in the voltage range of 1.6–4.0 V at a specific current of 117 mA g^{-1} (C/3 rate). The lower specific capacity shown by the full-cell system was due to the higher mass of the graphite negative electrode and, therefore, a rather high irreversible capacity "loss". Note that: 1) the graphitic anode thickness and density was not optimised, and 2) the SEI formation on the graphite is a major factor for high irreversible capacity "loss" during the first electrochemical Li^+ insertion into graphite materials.[38–40] This capacity "loss" means that a significant fraction of the lithium from the oxide was immobilised at the carbon electrode and, therefore, not available for full charging of the oxide electrode.

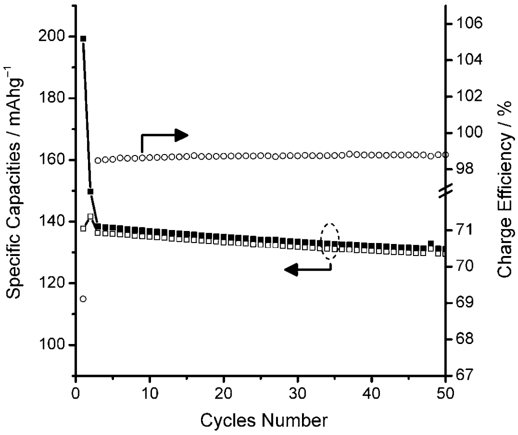

Figure 9. Cycle life behaviour of the $Li_4V_3O_8$ electrode (50 wt% active mass) in a full-cell (vs. graphite) system when cycled in the voltage range between 1.6 and 4.0 V. The specific current applied was 117 mA g^{-1} (C/3 rate). (■ charge, □ discharge, ○ charge efficiency).

To demonstrate the significance of the electrochemical redox contribution in the high voltage region (> 3.3 V), cyclic voltammetry (CV) measurements of the $Li_4V_3O_8$ electrodes in a full-cell system (vs. LBG1025 graphite) were carried out for two different cut-off cell voltages for charging, that is, 3.3 and 4.0 V, as shown in Figure 10. Note that the initial cell voltages ($U_{initial}$, which is equivalent to the potential difference between the anode and cathode) were quite similar in both cases, that is, approximately −0.4 V. A negative cell voltage was observed due to the lower open circuit potential for the over-lithiated vanadates (≈2.6 V vs. Li/Li^+) when compared to the open circuit potential for the fresh graphitic anodes (≈3.0 V vs. Li/Li^+). The broad redox peak pair above 3.3 V (see Figure 10b) represents the deep Li^+ insertion/de-insertion from the $Li_{1+x}V_3O_8$ ($0.02 < x < 0.32$) cathode.[41,42] In addition, a small anodic peak (≈2.04 V) was observed for both full cells, which corresponds to the solid electrolyte interphase (SEI) film formation process for the graphitic anode during the first charge of the cell.[38–40] This led to the presence of an irreversible capacity "loss" during the first cycle and also resulted in the shifting of the redox peak pair during the subsequent charge-discharge cycles, as confirmed in Figure 11. However, there was no major capacity decrease, as observed from the peak intensities, even when cycled up to 10 cycles. This shows that the $Li_4V_3O_8$ cathode is a structurally stable compound with outstanding ruggedness towards Li^+ insertion/de-insertion.[30–33]

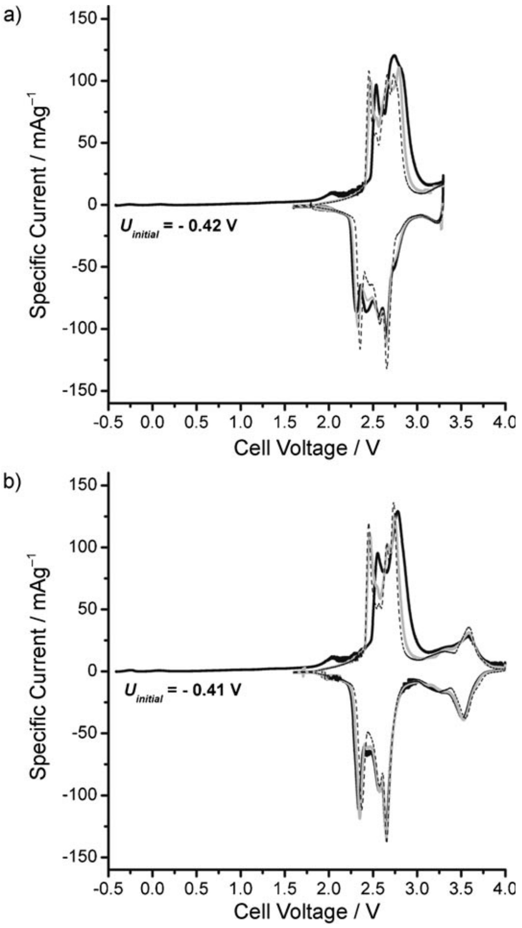

Figure 10. Cyclic voltammograms (CVs) of the $Li_4V_3O_8$ electrodes (50 wt% active mass) in a full-cell (vs. graphite) system when cycled at different cut-off voltages: a) 1.6–3.3 V, and b) 1.6–4.0 V. The scan rate applied was 0.1 mV s^{-1}. Note that the initial cell voltage is given by $U_{initial}$. (——: first cycle, ——: second cycle, – – –: 10th cycle).

Conclusion

$Li_4V_3O_8$ materials have been successfully prepared through chemical lithiation by Li_2S of spherical $Li_{1.1}V_3O_8$ precursor materials obtained from the spray-drying technique. The $Li_4V_3O_8$ materials are stable in air up to 5 h, with almost no capacity drop for the samples stored under air. Prolonged

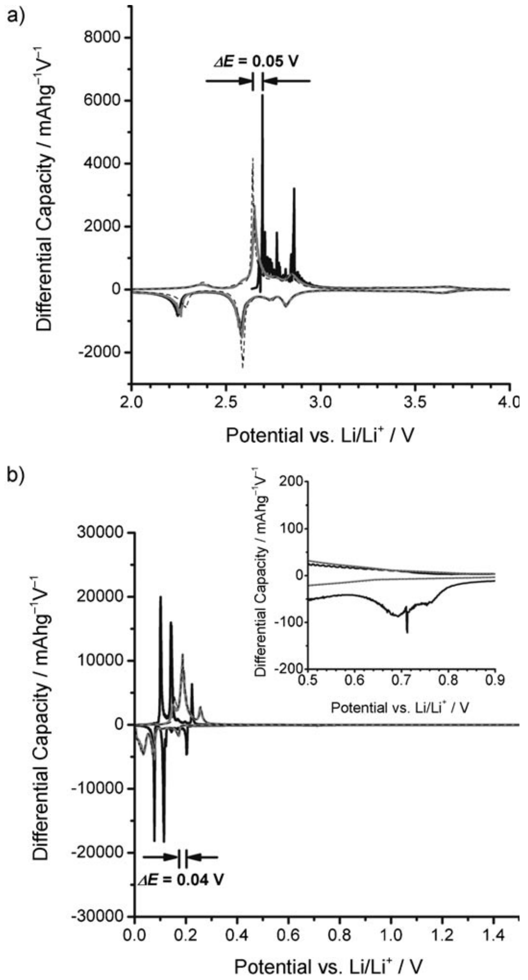

Figure 11. Differential capacity plots of the individual working electrodes when cycled against a Li metal counter electrode: a) $Li_4V_3O_8$ and b) LBG1025 graphite. The enlarged plot for (b) is shown in the inset, revealing a reduction peak corresponding to the SEI formation during the first charge. Note that the peak shift between the first and second cycle is given by the voltage difference as ΔE, for both working electrodes. (——: first cycle, ——: second cycle, – – –: 10th cycle).

exposure of these over-lithiated vanadates in ambient air leads to surface oxidation, converting $Li_4V_3O_8$ into the monoclinic phase $Li_{1.1}V_3O_8$ and the electrochemically inert Li_2CO_3. When sufficient carbon black is added, the $Li_4V_3O_8$ electrode exhibits good cycling behaviour and excellent rate capabilities, matching those of the $Li_{1.1}V_3O_8$ precursor material, that is, retaining an average charge capacity of 205 mAh g^{-1} at 2800 mA g^{-1} (8C rate) when cycled in the potential range of 2.0–4.0 V versus Li metal. When applied in a non-optimised full-cell system (vs. graphite), the $Li_4V_3O_8$ electrode shows promising cycling behaviour, retaining a charge capacity above 130 mAh g^{-1} beyond 50 cycles when cycled in the voltage range of 1.6–4.0 V at a specific current of 117 mA g^{-1} (C/3 rate). We believe that with further synthetic optimizations (increasing the degree of lithiation and/or changing the morphology of the compound) and better balancing of the electrodes' masses and densities (especially for the graphitic anode), $Li_4V_3O_8$ should be a viable candidate as a high capacity cathode material in commercial lithium-ion batteries.

Experimental Section

Material synthesis: The $Li_{1.1}V_3O_8$ precursor material was synthesised through a spray-drying process in air using a Mobile Minor 2000 type device, followed by heat treatment in air at 320 °C for 1 h.[17] $Li_4V_3O_8$ was prepared through reduction of this $Li_{1.1}V_3O_8$ precursor material by Li_2S (Alfa-Aesar) under a dry nitrogen gas atmosphere. The reactants, with molar ratio of Li/V (1.45/1), were heated under reflux in anhydrous acetonitrile (99.99 %, Merck, Germany) at 80 °C for 24 h.[18] It is important to note that there should be no reaction between the $Li_{1.1}V_3O_8$ and the anhydrous acetonitrile solvent. Therefore, any possible V dissolution during this step would be negligible and should have no bearing on the electrochemical properties of the final product, because the amount of lithiation was calculated using ICP-OES based on the final dried product. The by-product, S, was afterwards washed out by a warm ($\approx$50 °C) ethanol/toluene (1/1 v/v) solvent mixture, used alternately; that is, first ethanol, then toluene, and so forth.

Material characterization: The as-synthesised $Li_4V_3O_8$ material was analyzed for lithium content using the atomic absorption spectroscopy (AAS) technique in the emission mode. The vanadium content was determined by a potentiometric titration technique.[18] The materials were analyzed by X-ray diffraction (XRD) using a Bruker "D4-Endeavor" equipped with a diffracted-beam monochromator (Cu-Kα radiation) in the 5–70° ($2\theta_{Cu}$) range using a 0.02° ($2\theta_{Cu}$) step of 3.6 s duration. The unit cell structural parameters were refined by the Rietveld method using the Fullprof/Winplotr software package.[43] Scanning electron microscopy (SEM) images were obtained using a JEOL JSM 6400F microscope. To avoid charge accumulation, a thin layer of Au/Pd was deposited by cathodic sputtering on the powders.

Electrochemical measurements: The $Li_4V_3O_8$ cathodes were prepared by a solvent route where anhydrous acetonitrile (99.99 %, Aldrich) was used as the dispersing medium. The $Li_4V_3O_8$ active material, carbon black (CB), and polymeric binder mixture (PVdF-HFP and PEO) were dispersed in the solvent under magnetic stirring for 1 h. The solvent quantity was 4 mL for every 500 mg of the composite materials. The as-prepared slurry was doctor-bladed on aluminium foil and dried in an argon-filled glove box. After drying, electrode disks (1.3 cm^2) were punched for test cell assembly. The working electrodes now consist of 50 wt % $Li_4V_3O_8$, 43 wt % carbon black (Super P, TIMCAL SA, Switzerland), and 7 wt % polymeric binder mixture (1:1 by weight of PVdF-HFP, Kynar 2801, Atochem) and PEO ($M_w = 300000$, Aldrich). The mass loading of the cathodes was typically 4–6 mg of active material per cm^2. Hermetically sealed laboratory test cells[44] were used in which the working and counter electrodes (the latter from metallic lithium for a half-cell, and from LBG1025 graphite (Superior Graphite Co., Switzerland) for a full cell) were slightly pressed together (at $\approx$2 kg cm^{-2}) against a glass fibre separator soaked with a standard battery electrolyte (1 M $LiPF_6$ in EC:DMC (1:1 by weight), Ferro GmbH). The electrochemical cycling was performed between 2.0–4.0 V (half-cell, vs. Li metal) or 1.6–4.0 V (full cell, vs. LBG1025 graphite) in the galvanostatic mode, immediately followed by a potentiostatic mode until the specific current decreased to 10 % of the current used in the galvanostatic mode. For determining the C-rate, a theoretical specific charge of 350 mAh g^{-1} of the vanadates was assumed for all cases. For the air sensitivity tests, the exposure time was calculated based on the duration of time for the doctor-bladed electrode exposed under ambient air. For the long-term cycling tests, the charge and discharge rates in the galvanostatic mode were equal to C/3 rate. For the rate capability tests, the specific current was varied from C/10 to 8C rates. For each C-rate an average value was calculated for the first 10 cycles only. Please note that all terms related to charge (Li^+ extraction) or discharge (Li^+ insertion) used throughout this paper were defined based on the standard lithium-ion battery full-cell configuration.

Acknowledgements

Technical assistance from Mr. W. Scheifele (PSI) and Mr. H. Kaiser (PSI) is highly appreciated. Scientific discussions with Dr. M. Holzapfel (PSI) are gratefully acknowledged. We would also like to thank Mr. M. Wissler (Superior Graphite Co., Switzerland) for the supply of the LBG1025 graphite sample.

---

[1] B. Scrosati, *Nature* **1995**, *373*, 557.
[2] J.-M. Tarascon, M. Armand, *Nature* **2001**, *414*, 359.
[3] M. S. Whittingham, *J. Electrochem. Soc.* **1976**, *123*, 315.
[4] S. H. Ng, S. Y. Chew, J. Wang, D. Wexler, Y. Tournayre, K. Konstantinov, H. K. Liu, *J. Power Sources* **2007**, *174*, 1032.
[5] D. W. Murphy, P. A. Christian, F. J. Disalvo, J. N. Carides, *J. Electrochem. Soc.* **1979**, *126*, 497.
[6] D. W. Murphy, P. A. Christian, F. J. Disalvo, J. N. Carides, J. V. Waszczak, *J. Electrochem. Soc.* **1981**, *128*, 2053.
[7] S. Y. Chew, C. Feng, S. H. Ng, J. Wang, Z. Guo, H. Liu, *J. Electrochem. Soc.* **2007**, *154*, A633.
[8] T. J. Patey, S. H. Ng, R. Büchel, N. Tran, F. Krumeich, J. Wang, H. K. Liu, P. Novák, *Electrochem. Solid-State Lett.* **2008**, *11*, A46–A50.
[9] C. Satto, P. Sciau, E. Dooryhee, J. Galy, P. Millet, *J. Solid State Chem.* **1999**, *146*, 103.
[10] M. S. Whittingham, M. B. Dines, *J. Electrochem. Soc.* **1977**, *124*, 1387.
[11] M. Baba, N. Kumagai, H. Kobayashi, O. Nakano, K. Nishidate, *Electrochem. Solid-State Lett.* **1999**, *2*, 320.
[12] S.-H. Lee, P. Liu, C. E. Tracy, D. K. Benson, *Electrochem. Solid-State Lett.* **1999**, *2*, 425.
[13] J. Barker, M. Y. Saidi, J. L. Swoyer, *J. Electrochem. Soc.* **2003**, *150*, A1267.
[14] L. A. de Picciotto, K. T. Adendorff, K. T. Liles, M. M. Thackeray, *Solid State Ionics* **1993**, *62*, 297.
[15] J. Kawakita, T. Miura, T. Kishi, *Solid State Ionics* **1999**, *120*, 109.
[16] S. Jouanneau, A. Verbaere, D. Guyomard, *J. Solid State Chem.* **2005**, *178*, 22.
[17] N. Tran, K. G. Bramnik, H. Hibst, J. Prölss, N. Mronga, M. Holzapfel, W. Scheifele, P. Novák, *J. Electrochem. Soc.* **2008**, *155*, A384.
[18] B. Chaloner-Gill, D. R. Shackle, T. N. Andersen, *J. Electrochem. Soc.* **2000**, *147*, 3575.
[19] S.-H. Ng, J. Wang, D. Wexler, K. Konstantinov, Z.-P. Guo, H.-K. Liu, *Angew. Chem.* **2006**, *118*, 7050; *Angew. Chem. Int. Ed.* **2006**, *45*, 6896.
[20] H. Gao, C. Y. Jiang, C. R. Wan, *J. Power Sources* **2004**, *125*, 90.
[21] A. D. Wadsley, *Acta Cryst.* **1957**, *10*, 261.
[22] K. Ozawa, *Solid State Ionics* **1994**, *69*, 212.
[23] J.-S. Shin, C.-H. Han, U.-H. Jung, S.-I. Lee, H.-J. Kim, K. Kim, *J. Power Sources* **2002**, *109*, 47.
[24] J. Vetter, M. Holzapfel, A Wuersig, W. Scheifele, J. Ufheil, P. Novák, *J. Power Sources* **2006**, *159*, 277.
[25] D. Guy, B. Lestriez, D. Guyomard, *Adv. Mater.* **2004**, *16*, 553.
[26] D. Guy, B. Lestriez, R. Bouchet, V. Gaudefroy, D. Guyomard, *Electrochem. Solid-State Lett.* **2005**, *8*, A17.
[27] D. Guy, B. Lestriez, R. Bouchet, V. Gaudefroy, D. Guyomard, *J. Power Sources* **2006**, *157*, 438.
[28] D. Guy, B. Lestriez, R. Bouchet, D. Guyomard, *J. Electrochem. Soc.* **2006**, *153*, A679.
[29] E. Ligneel, B. Lestriez, O. Richard, D. Guyomard, *J. Phys. Chem. Solids* **2006**, *67*, 1275.
[30] S. Panero, M. Pasquali, G. Pistoia, *J. Electrochem. Soc.* **1983**, *130*, 1225.
[31] G. Pistoia, S. Panero, M. Tocci, R. V. Moshtev, V. Manev, *Solid State Ionics* **1984**, *13*, 311.
[32] G. Pistoia, M. Pasquali, M. Tocci, R. V. Moshtev, V. Manev, *J. Electrochem. Soc.* **1984**, *132*, 281.
[33] G. Pistoia, M. Pasquali, M. Tocci, R. V. Moshtev, V. Manev, *J. Power Sources* **1985**, *15*, 13.
[34] J. Kawakita, T. Miura, T. Kishi, *J. Power Sources* **1999**, *83*, 79.
[35] S. Jouanneau, A. Le Gal La Salle, A. Verbaere, D. Guyomard, *J. Electrochem. Soc.* **2005**, *152*, A1660.
[36] A. M. Kannan, A. Manthiram, *J. Power Sources* **2006**, *159*, 1405.
[37] G. Gritzner, G. Kreysa, *Pure Appl. Chem.* **1993**, *65*, 1009.
[38] P. Novák, W. Scheifele, M. Winter, O. Haas, *J. Power Sources* **1997**, *68*, 267.
[39] J. S. Gnanaraj, Y. S. Cohen, M. D. Levi, D. Aurbach, *J. Electroanal. Chem.* **2001**, *516*, 89.
[40] J. Shim, K. A. Striebel, *J. Power Sources* **2003**, *119–121*, 934.
[41] N. Dupré, J. Gaubicher, D. Guyomard, C. P. Grey, *Chem. Mater.* **2004**, *16*, 2725.
[42] F. Boucher, N. Bourgeon, K. Delbé, P. Moreau, D. Guyomard, G. Ouvrard, *J. Phys. Chem. Solids* **2006**, *67*, 1238.
[43] T. Roisnel, J. Rodriguez-Carvajal, *Mater. Sci. Forum* **2001**, *378–381*, 118.
[44] P. Novák, W. Scheifele, F. Joho, O. Haas, *J. Electrochem. Soc.* **1995**, *142*, 2544.

Received: February 15, 2008
Revised: July 3, 2008